The Plant Journal (2004), **39**, 403–414 doi: 10.1111/j.1365-313X.2004.02128.x

Arabidopsis Yellow Stripe-Like2 (*YSL2*): a metal-regulated gene encoding a plasma membrane transporter of nicotianamine–metal complexes

Raymond J. DiDonato Jr[1], Louis A. Roberts[†], Tamara Sanderson, Robynn Bosler Eisley and Elsbeth L. Walker[*]
Biology Department, University of Massachusetts, Amherst, MA 01003, USA, and
[1]Microbiology Department, University of Massachusetts, Amherst, MA 01003, USA

Received 23 January 2004; revised 26 April 2004; accepted 28 April 2004.
[*]For correspondence (fax +1 413 545 3243; e-mail ewalker@bio.umass.edu).
[†]Current address: Louis A. Roberts, Biomedical Research Institute, Baystate Medical Center, Springfield, MA 01199, USA.

Summary

The Yellow Stripe-Like (YSL) family of proteins has been identified based on sequence similarity to maize Yellow Stripe1 (YS1), the transporter responsible for the primary uptake of iron from the soil. YS1 transports iron that is complexed by specific plant-derived Fe(III) chelators called phytosiderophores (PS). Non-grass species of plants neither make nor use PS, yet YSL family members are found in non-grass species (monocot, dicot, gymnosperm, and moss species) including *Arabidopsis thaliana*. YSLs in non-grasses have been hypothesized to transport metals complexed by nicotianamine (NA), an iron chelator that is structurally similar to PS and which is found in all higher plants. Here we show that *Arabidopsis* YSL2 (At5g24380) transports iron and copper when these metals are chelated by NA. *YSL2* is expressed in many cell types in both roots and shoots, suggesting that diverse cell types obtain metals as metal–NA complexes. *YSL2* transcription is regulated by the levels of iron and copper in the growth medium. Based on its expression pattern, a major function of the YSL2 appears to be in the lateral movement of metals in the vasculature.

Keywords: nicotianamine, iron, copper, YS1, *Arabidopsis*, membrane protein.

Introduction

Plants, like all organisms, achieve metal ion homeostasis in several ways. The first is by controlling primary uptake so that adequate but non-toxic amounts of metal ions are acquired from the soil. Our understanding of the mechanisms of primary uptake has improved rapidly in recent years, especially for the uptake of iron and zinc (Curie *et al.*, 2001; Eide *et al.*, 1996; Grotz *et al.*, 1998; Henrique *et al.*, 2002; Lasat *et al.*, 2000; Pence *et al.*, 2000; Robinson *et al.*, 1999; Varotto *et al.*, 2002; Vert *et al.*, 2002). Another homeostatic mechanism is sequestration of excess metals to prevent them from causing oxidative damage to cells. A number of such homeostatic mechanisms have been described, for example, the metallothioneins, phytochelatins (recently reviewed by Cobbett and Goldsbrough, 2002) and ferritin (reviewed by Briat *et al.*, 1999) all serve to sequester metals intracellularly. A vacuolar Nramp protein responsible for remobilization of vacuolar metal stores has recently been described (Thomine *et al.*, 2003).

Although no less important than uptake and sequestration, the mechanisms controlling the correct distribution of metals into particular organs, tissues and cells of the plant have received less attention. Because many metals are highly reactive, long-distance movement probably involves relatively non-reactive complexed or chelated metals. For example, an iron transport protein that appears to carry iron during phloem movement has recently been described (Kruger *et al.*, 2002). The processes of metal ion partitioning on the whole plant level are not well characterized, and the molecular mechanisms by which metal ions are moved throughout the plant body have not been examined in detail.

The non-proteinogenic amino acid nicotianamine (NA) appears to play a key role in metal partitioning in plants. Nicotianamine is a strong complexor of various transition metals, particularly Fe(II) (Anderegg and Ripperger, 1989) and Fe(III) (von Wiren *et al.*, 1999), as well as Cu(II), Ni(II), Co(II), Mn(II) and Zn(II) (Anderegg and Ripperger, 1989).

Fe(II)–NA complexes are relatively inactive Fenton reagents, and so complexation of iron by NA has been proposed as a means by which plants control oxidative damage by iron during transport (Reichman and Parker, 2002; von Wiren *et al.*, 1999). NA is present in shoots and roots at concentrations ranging between 20 and 500 nmol g^{-1} fresh weight (Stephan *et al.*, 1990), and is present in both xylem (approximately 20 μM; Pich and Scholz, 1996) and phloem (approximately 130 μM; Schmidke and Stephan, 1995), suggesting that NA is a major complexor of metals throughout the plant.

Much of our understanding of the physiologic function of NA comes from the complex phenotype of a tomato mutant called *chloronerva*. The *chloronerva* mutation disrupts the function of the single gene in tomato encoding NA synthase (Herbik *et al.*, 1999; Higuchi *et al.*, 1999; Ling *et al.*, 1999). Homozygous *chl* plants exhibit symptoms of iron deficiency: interveinal chlorosis in young leaves and upregulation of the iron acquisition system (extrusion of protons into the medium and increased ferric reductase activity; Pich and Scholz, 1991; Stephan and Grun, 1989). Mature leaves do become fully green, albeit slowly, probably because iron begins to arrive via xylem once the leaf matures fully and transpiration occurs at sufficient rates. The levels of iron, zinc, manganese and copper are all below normal in shoot apices, which rely on phloem transport for their nutrient supply (Pich *et al.*, 1994). This, together with the deficiency symptoms in young tissues, has led to the conclusion that NA is required for phloem transport of these metals.

In contrast to the metal deficiency of young tissues in *chl* mutants, measurements of metal concentration in mature tissues indicate that excess iron, zinc and manganese (Pich *et al.*, 1994) are accumulated. Thus, NA does not appear to be required for either primary uptake or xylem translocation of these metals. Most of the excess iron that is transported to mature leaves in *chloronerva* plants is symplasmic, indicating that iron unloaded from the xylem is taken up by leaf cells in the absence of NA (Becker *et al.*, 1992). However, the high concentration of iron in leaf cells leads to the formation of intracellular precipitates (Becker and Manteuffel, 1995; Liu *et al.*, 1998). The presence of these precipitates has been interpreted as an indication that NA is required for maintaining the solubility of intracellular iron pools, but it is difficult to separate the effect of high overall concentrations of iron from the effect of the absence of NA.

Although NA may not be necessary for root-to-shoot translocation of iron, zinc and manganese, it does appear to be required for translocation of copper to shoots. Homozygous *chloronerva* mutant plants have excess copper in their roots, but fail to transport normal amounts of copper to mature leaves. Furthermore, xylem exudates from mutant plants contain unusually low levels of copper (Pich and Scholz, 1996). Based on physical measurements, von Wiren *et al.* (1999) predicted that, in wild-type plants, 100% of the copper in the xylem would occur as NA complexes.

Recently, a family of proteins called Yellow Stripe-Like (YSL) was suggested to transport metals bound to NA (Curie *et al.*, 2001). This suggestion was based on the sequence similarity between the *YSL* genes deduced from the *Arabidopsis thaliana* genome sequence and the recently cloned *Yellow Stripe1* gene from maize (*ZmYS1*). YS1 is a proton-coupled symporter (Schaaf *et al.*, 2003) that transports iron complexed by specific plant-derived Fe(III) chelators known as phytosiderophores (PS) that form stable Fe(III) chelates (Curie *et al.*, 2001; Roberts *et al.*, 2004; Schaaf *et al.*, 2004). NA is the direct biochemical precursor to PS, and as such, is structurally similar. Recently, ZmYS1 was shown to transport iron from Fe(II)–NA complexes (Roberts *et al.*, 2004; Schaaf *et al.*, 2004), and was observed to transport metals other than iron (Schaaf *et al.*, 2004). Because PS are neither made nor used by non-grass species like *Arabidopsis*, the role of the YSL proteins in *Arabidopsis* is likely in the transport of metals complexed by the PS-related compound NA.

Here, we examine *Arabidopsis* YSL2 (At5g24380) and find that, as predicted, this protein transports metals that are chelated by NA. Like ZmYS1, *Arabidopsis* YSL2 transports both iron and copper when these metals are complexed with NA. In contrast to ZmYS1, YSL2 transports only Fe(II), and can also transport copper from Cu–NA, which is not a suitable substrate for copper transport by ZmYS1. The pattern of expression of YSL2 indicates that the transport of metal–NA occurs in diverse cell types in both roots and shoots, suggesting that metals are regularly imported into cells as NA complexes. Consistent with its function as an iron and copper transporter, *YSL2* transcription is regulated by the levels of these metals in the growth medium. YSL2 has an unusual pattern of distribution within the plasma membranes of vascular parenchyma cells that is consistent with a function in moving metals laterally within veins. Based on its expression pattern, the major function of YSL2 appears to be in the lateral movement of metals within the vasculature. This movement appears to be most critical when iron is abundantly available, as *YSL2* expression under iron-deficient growth conditions is reduced.

Results

Cloning of a YSL2 *cDNA and functional complementation in yeast*

Eight full-length *YSL* genes (*AtYSL*s) can be identified in the *Arabidopsis* genome. (A ninth partial gene is also evident.) The AtYSL proteins inferred from cloned YSL cDNAs (Roberts and Walker, unpublished data, Genbank accession numbers AY515560, AY515561, AY515562, AY515563, AY515564, AY515565, AY515566), or inferred from the *Arabidopsis* genome sequence share strong full-length sequence similarity with each other and with the YS1 protein

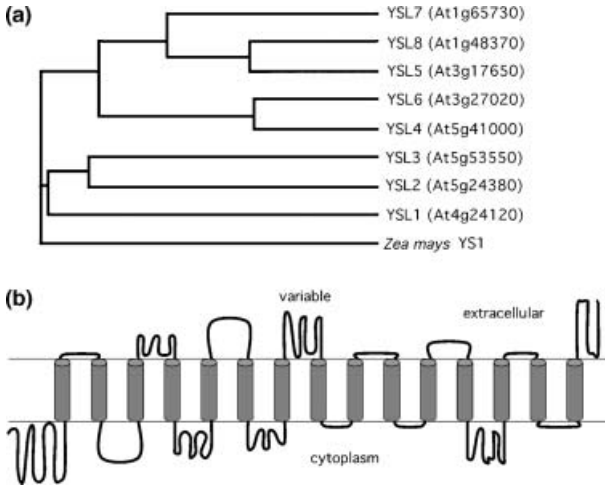

Figure 1. The *Arabidopsis* YSL family of proteins.
(a) Clustal analysis of AtYSL protein sequences.
(b) Consensus-predicted topology for the YSL family generated using TMAP (Persson and Argos, 1994, 1996).

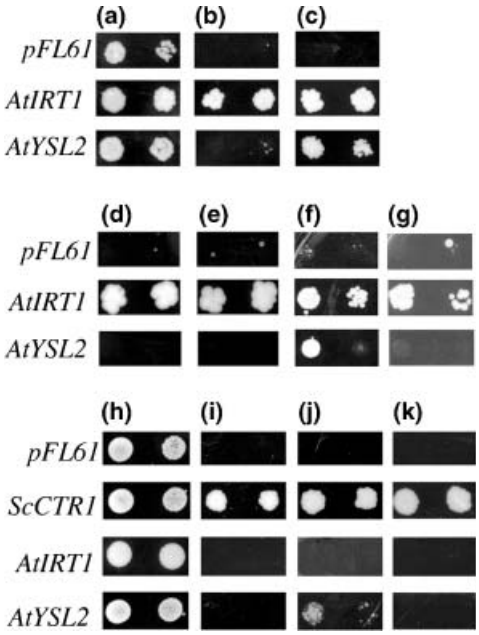

Figure 2. Functional complementation of yeast.
(a–g) The *fet3fet4* strain DEY1453 was transformed with constructs expressing *YSL2*, *AtIRT1*, or the empty vector, *pFL61*, and grown on synthetic defined medium containing: (a) 50 μM iron citrate; (b) 4 μM Fe(II)SO_4; (c) 4 μM Fe(II)SO_4 with 5 μM NA; (d) 10 μM Fe(III)Cl_3; (e) 10 μM Fe(III)Cl_3 with 10 μM MA; (f) 10 μM Fe(II)SO_4 with 10 μM MA; (g) 10 μM Fe(III)Cl_3 with 10 μM NA.
(h–k) The *ctr1* strain YSC5 was transformed with constructs expressing *YSL2*, *AtIRT1*, *ScCTR1* or the empty vector, *pFL61*, and grown on synthetic defined medium containing: (a) glucose and 1 μM $CuSO_4$; (b) glycerol and 1 μM $CuSO_4$; (c) glycerol and 1 μM $CuSO_4$ with 5 μM NA; (d) glycerol and 1 μM $CuSO_4$ with 10 μM MA. Pairs of spots correspond to 10- and 100-fold dilutions of the original cultures.

from maize (ZmYS1). Clustal analysis of AtYSL protein sequences (Figure 1a) indicates the existence of three distinct sub-groups within the family. A consensus topology for the nine YSL family members (eight AtYSLs and one ZmYS1) was generated using TMAP (Persson and Argos, 1994, 1996). There are 15 predicted transmembrane domains (Figure 1b). Among the predicted extra-membranous segments of the proteins is one region with very poor sequence conservation (the variable region). Another variable region is found at the amino termini of the proteins. However, in spite of poor sequence similarity, the amino acid composition of the amino termini of all nine YSLs is strikingly similar, being unusually rich in the acidic residues glutamate and aspartate.

The AtYSL protein that is most similar to ZmYS1 is YSL2 (At5g24380; 62% identical and 78% similar to ZmYS1). Because of this strong sequence similarity, the *YSL2* gene was chosen for further study. A cDNA corresponding to the full coding region of *YSL2* was obtained by screening a size-selected hypocotyl cDNA library (Genbank AY515561; see Experimental procedures). This *YSL2* cDNA was subcloned into the yeast expression vector *pFL61* (Minet *et al.*, 1992) for use in yeast functional complementation assays.

To test whether YSL2 is able to transport iron–NA, we used the iron-uptake-defective yeast strain DEY1453 (*fet3fet4* double mutant). This strain cannot grow on iron-limited medium. The YSL2 cDNA was introduced into DEY1453, and growth was tested on a medium containing micromolar amounts of iron with and without NA (Figure 2). As a positive control, the *Arabidopsis* IRT1 cDNA, which is capable of supporting the growth of the *fet3fet4* yeast (Eide *et al.*, 1996), was also introduced into the strain. The viability of each strain is demonstrated by growth under permissive conditions (50 μM iron citrate, pH 4.2; Figure 2a). Expression of IRT1 restored growth under all conditions, as expected. Expression of the *YSL2* cDNA restored growth on 4 μM Fe(II)–NA, but not on 4 μM Fe(II) in the absence of NA (Figure 2b,c). This result indicates that YSL2 is an iron transporter that can use NA-bound Fe(II) as a substrate.

As a further test of the substrate specificity of YSL2, growth assays were performed using iron-phytosiderophore as a substrate. Non-grass species do not synthesize PS, and so these conditions are not intended to mimic physiologic conditions in *Arabidopsis*. Instead, the question is whether YSL2 requires NA *per se*, or can instead use the structurally similar but non-identical compound, mugineic acid (MA). Iron was provided as Fe(III)–MA, which is the substrate for the maize YS1 transporter (Curie *et al.*, 2001), or as Fe(II)–MA, which is not expected to be formed in natural soil conditions where iron is rapidly oxidized. YSL2 did not complement growth on 10 μM Fe(III)Cl_3, 10 μM Fe(III)–MA, or 10 μM Fe(III)–NA (Figure 2d,e,g), indicating that Fe(III) is a poor substrate for transport by YSL2, even in the presence of NA. Interestingly, YSL2 did complement growth on a 4 μM Fe(II)–MA-containing medium (Figure 2f). This result

indicates that YSL2 requires Fe(II) as a substrate for uptake, but is able to accept iron from two related, yet non-identical chelators.

To test for copper uptake, yeast strain YSC5 (*ctr1*), was used. The YSC5 strain is unable to take up adequate amounts of copper because of the deletion of the *CTR1* gene encoding the yeast high-affinity copper transporter. The growth assay to test copper uptake is complicated by the fact that, in yeast, iron uptake depends on adequate intracellular levels of copper (Askwith *et al.*, 1994; Dancis *et al.*, 1994b). As a result, under ordinary conditions, the growth defect exhibited by YSC5 yeast is caused by secondary failure to take up iron, not the primary copper uptake defect. Clearly, growth defects related to inadequate iron uptake could potentially be reversed through expression of YSL2. To test directly for copper uptake, glycerol was substituted for glucose in the medium, requiring the cells to respire, which in turn leads to an absolute requirement for copper (Dancis *et al.*, 1994a; Zhou and Gitschier, 1997). Thus, inadequate copper uptake restricts the growth of the *ctr1* strain on medium containing glycerol as the sole carbon source.

The plasmids expressing YSL2 and control cDNAs were introduced into the *ctr1* yeast. The positive control was the yeast high-affinity copper transporter *CTR1*. *AtIRT1*, which does not transport copper but does transport iron (Eide *et al.*, 1996), is a negative control in these experiments that would reveal restoration of growth resulting from alleviation of iron deficiency. The viability of each strain is demonstrated by growth under permissive conditions (SD-URA with glucose; Figure 2h). Under the restrictive growth conditions used in this assay (1 μM $CuSO_4$ or 1 μM $CuSO_4$ with 5 μM NA), only the *CTR1* positive control and the *YSL2* cDNA were able to restore growth. Growth restoration by YSL2 required NA in the medium (Figure 2i,j). The ability of *YSL2* to complement on copper complexed with the phytosiderophore, MA was also tested. Under the conditions used in this experiment (1 μM $CuSO_4$, 5 μM MA), MA was not able to substitute for NA in the uptake of copper by YSL2 (Figure 2k). This result indicates that, in addition to being a transporter of iron, YSL2 is also a copper transporter that requires Cu–NA as the substrate for transport.

We also tested whether expression of YSL2 could restore growth of a zinc-uptake-defective strain of yeast [ZHY3 (Zhao and Eide, 1996); *zrt1zrt2*]. No complementation by *YSL2* was observed on a medium with 1.4 μM $ZnSO_4$ either containing or lacking NA (not shown), suggesting that YSL2 does not transport zinc at the low, physiologic concentration used in our experiments.

Pattern of YSL2 *expression*

To establish the pattern of expression of *YSL2*, we used a semi-quantitative RT-PCR assay. RNA was isolated from the leaves, roots, flowers, siliques, and inflorescence stems of 3-week-old plants. *YSL2* mRNA was detected predominantly in the leaf and root tissues of 3-week-old plants, although expression was also detectable at low levels in the stem, cauline leaves, flowers, and siliques (not shown). In order to refine these observations, we made β-glucuronidase (GUS) reporter constructs containing the upstream sequences of *YSL2* fused in-frame to GUS (*YSL2p:GUS*). This construct contains 564 bp of *YSL2* promoter plus 155 bp of 5′ UTR sequence and 13 nucleotides (four amino acids) of coding sequence. In shoots, *YSL2p:GUS* was most strongly expressed in fully expanded leaves, while young, still-growing leaves expressed only weakly or not at all (Figure 3a). In leaf tissues, *YSL2p:GUS* was expressed most strongly in the vasculature, but weaker expression was also observed in non-vascular tissues, especially in cells close to the leaf veins (Figure 3b,c). Transverse sections through the midveins showed that *YSL2p:GUS* was expressed in xylem-associated cells and the mesophyll (Figure 3c).

In roots, the *YSL2* promoter conferred GUS expression in the apical end of the elongation zone (Figure 3e). *YSL2p:GUS* expression continued throughout the rest of the root up to the root/shoot junction (Figure 3d). No GUS expression was observed in the meristematic zones or the root cap (Figure 3e). *YSL2p:GUS* was most strongly expressed in the vascular tissue of the primary root, but every cell type within the mature primary root stained positive for GUS activity (Figure 3f). Lateral roots recapitulate this pattern of expression. Thus, the *YSL2* promoter used in *YSL2p:GUS* confers broad expression throughout the root.

As RT-PCR analysis revealed expression in flowers and siliques, *YSL2p:GUS* expression was also examined in these structures. *YSL2p:GUS* was expressed in the vasculature of sepals, petals, anthers, and developing siliques (not shown). No *YSL2p:GUS* expression was observed in developing seeds. Expression was also observed in the stigma. Thus, the *YSL2* promoter used in *YSL2p:GUS* confers expression in many floral organs, implying that movement of NA-bound metals occurs within flowers and developing fruits.

YSL2 *expression is altered in response to metal deficiency*

To determine whether *YSL2* expression changes in response to metal deficiency, plants were grown on a 1X MS medium containing standard micronutrient amounts for a period of 7 days after germination (d.a.g.), then transferred to medium that lacked iron. Control plants were transferred to fresh plates containing standard MS. No special measures were taken to deplete minute amounts of metals contaminating either purified water or other reagents, so the medium undoubtedly contained trace amounts of metal. After 5 days on a metal-limited medium, RNA was prepared from shoots and roots and the relative steady state expression level of *YSL2* was

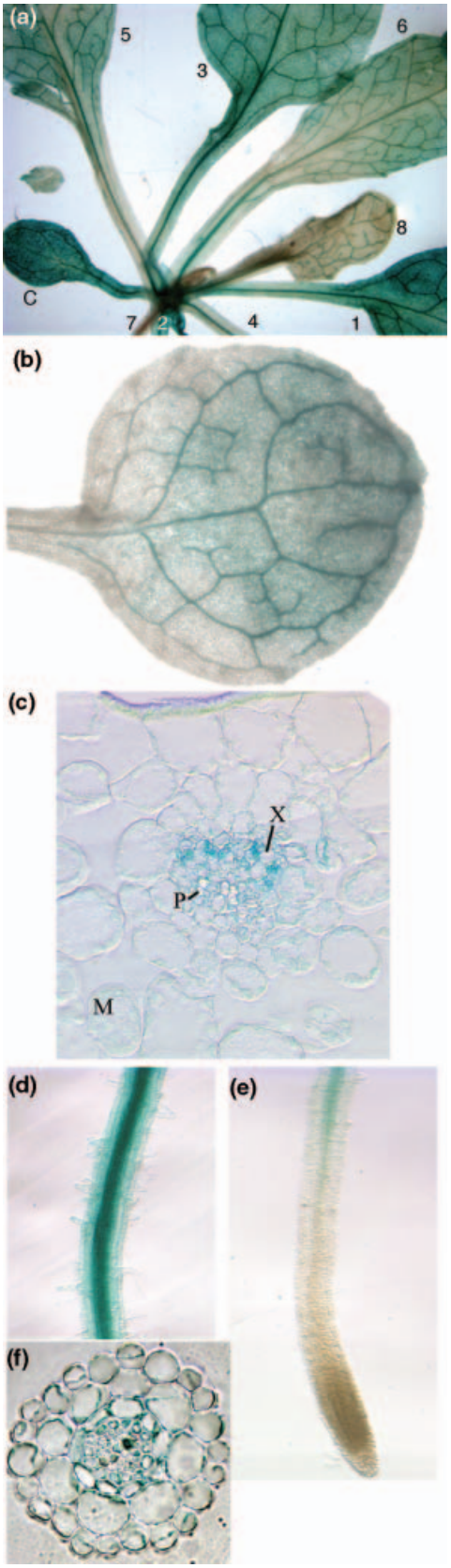

determined by semi-quantitative RT-PCR (Figure 4a). In response to limitation for iron, *YSL2* steady state mRNA expression was reduced in both shoots and roots. This pattern is in contrast to that observed for the primary *Arabidopsis* iron uptake transporter *IRT1* (Curie *et al.*, 2001; Eide *et al.*, 1996), which showed root-specific expression that was positively regulated by iron deficiency (Figure 4a). Regulation of YSL2 mRNA levels by copper starvation was also tested by growing plants on a complete medium and then shifting to a medium lacking copper for 5 days. No change in YSL2 mRNA expression was observed (not shown). It is important to note, however, that because special measures were not taken to ensure complete copper depletion of the medium, we cannot be certain that these plants were truly experiencing copper limitation.

Metal regulation of the YSL2 *promoter*

To ascertain whether regulation of *YSL2* occurs at the level of transcription, we examined *YSL2p:GUS* transgenic plants grown under iron-limited conditions. *YSL2p:GUS* plants were grown for 7 d.a.g. on standard MS medium, then transferred to iron-deficient medium for 5 days. GUS expression was monitored by histochemical staining (Figure 4b,c) and as GUS activity in protein extracts (Figure 4d). GUS activity from *YSL2p:GUS* in both shoots and roots was negatively affected by iron starvation. These results are consistent with the results from the RT-PCR analysis of the native *YSL2* gene, and suggest that this negative regulation is, at least in part, a function of the *YSL2* promoter. As the *YSL2p:GUS* transgene includes 155 bp of the *YSL2* 5′ UTR, it is also possible that post-transcriptional regulation occurring through this region is responsible for the changes in expression that are observed upon iron starvation.

Although YSL2 appeared to transport copper, copper deficiency had no apparent effect on *YSL2* mRNA expression. To investigate the effect of copper oversupply on expression of *YSL2*, we grew wild-type *Arabidopsis* Col0 plants for 10 d.a.g. on a standard 1X MS medium or on a 1X MS medium supplemented with 50 μM copper sulfate. Under the high copper conditions, plants showed symptoms of toxicity: decreased growth and yellowing of the leaves by day 7 of the copper treatment. RNA was prepared from leaves and roots of these plants, and was used as template for RT-PCR. Under high copper treatment, steady state *YSL2*

Figure 3. *YSL2p:GUS* expression. Transgenic lines containing *YSL2p:GUS* were examined for GUS activity by histochemical staining.
(a) 14 d.a.g. plate-grown *Arabidopsis*. Note darker staining in older leaves.
(b) A mature leaf from a 21 d.a.g. soil-grown plant.
(c) Transverse leaf section from a 21 d.a.g. *Arabidopsis* rosette leaf. Staining was carried out for a limited time period to highlight vascular staining relative to staining in other cells.
(d, e) Root mature and elongation zones and primary root tip.
(f) Transverse section of a root from 10 d.a.g. plate-grown plant.

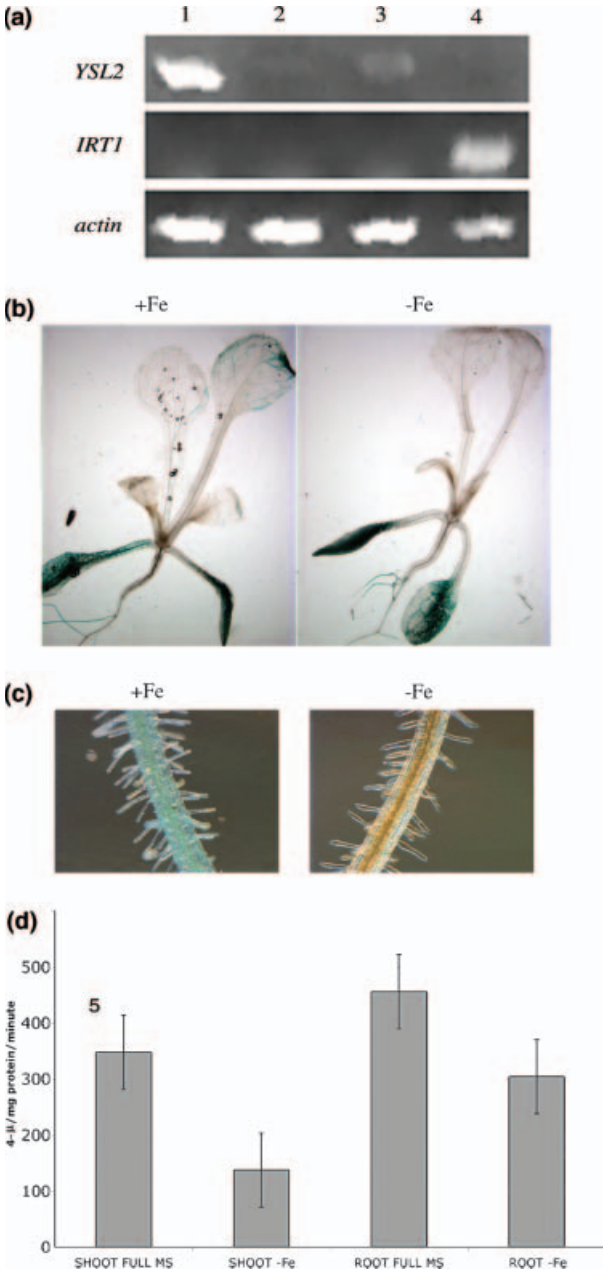

Figure 4. Effect of iron status on *YSL2* expression. Plants were grown 7 d.a.g. and transferred to iron-deficient medium for 5 days.
(a) Total RNA from: lane 1: shoots of plants grown in full metal conditions; lane 2: shoots of plants grown in iron-deficient conditions; lane 3: roots of plants grown in full metal conditions; lane 4: roots of plants grown in iron-deficient conditions, was reverse transcribed and the resulting cDNA was amplified by PCR with primers specific to *YSL2, IRT1* or *actin*.
(b, c) Shoot (b) and root (c) expression of *YSL2p:GUS* in plants grown under iron-sufficient (left) or iron-deficient (right) conditions.
(d) GUS activity in protein extracts of roots and shoots of plants grown with (full MS) and without iron (–Fe).

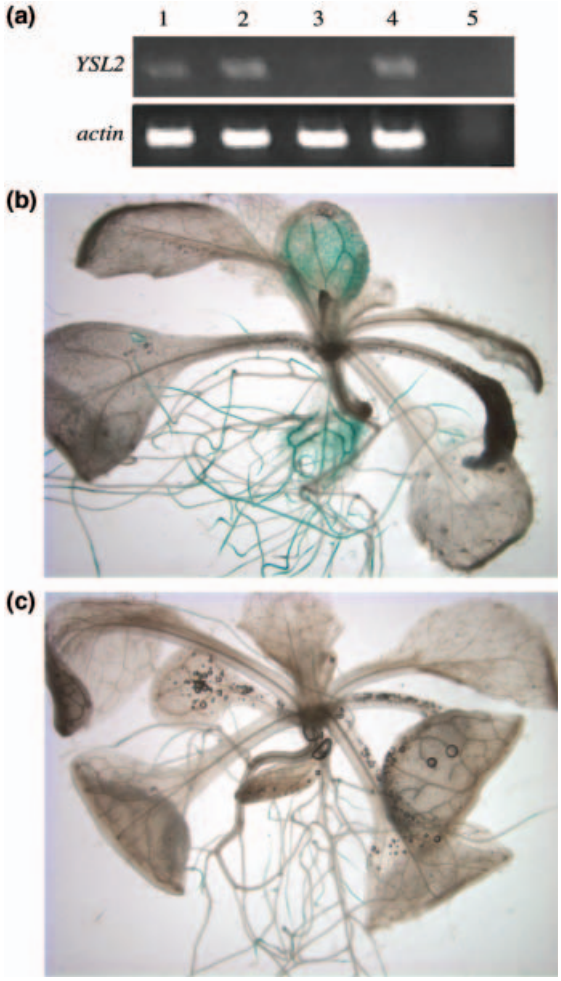

Figure 5. Effect of elevated copper on *YSL2* expression. Plants were grown 10 d.a.g. in the presence or absence of 50 μM $CuSO_4$.
(a) Total RNA from shoot (lanes 1 and 3) and root tissue (lanes 2 and 4) from plants grown under normal (lanes 1 and 2) or high copper (lanes 3 and 4) conditions was reverse transcribed and amplified by PCR. As a control for contaminating genomic DNA, a sample of RNA with no reverse transcription step (–RT) was also amplified (lane 5). The cDNA was amplified using primers specific to *YSL2* or to *actin*.
(b, c) *YSL2p:GUS* expression in plants grown under normal metal (b) or high copper (c) conditions.

mRNA abundance declined to barely detectable levels in shoots (Figure 5a, lanes 1 and 3) but appeared unchanged in roots (Figure 5a, lanes 2 and 4).

We examined *YSL2p:GUS* transgenic plants grown in conditions of copper excess identical to those used for the RT-PCR analysis (see above). GUS expression from *YSL2p:GUS* was markedly reduced in the copper-treated plants (Figure 5b,c). After only 2 h of GUS staining, untreated plants exhibited obvious GUS staining in both the roots and shoots, while the copper-treated plants exhibited little GUS activity in either tissue. The finding that copper treatment affected *YSL2p:GUS* expression in both the roots and shoots was surprising, because RT-PCR analysis of native gene expression had indicated that *YSL2* mRNA levels were decreased in shoots but not in roots. The inconsistency between the native mRNA abundance and GUS expression

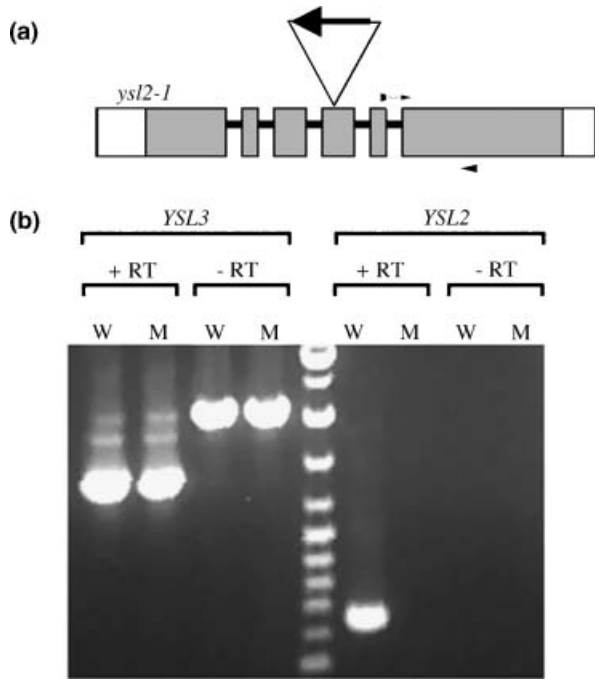

Figure 6. Identification of a T-DNA insertion in *YSL2*.
(a) Map of *ysl2-1* indicating the position (above) and orientation (arrow) of the T-DNA within the fourth exon of the *YSL2* gene. Introns are indicated as black lines; exons as boxes, with coding portions in gray and non-coding regions in white. Positions of RT-PCR primers are shown by small arrowheads above and below. The forward primer spans an intron/exon boundary.
(b) RT-PCR analysis of *ysl2-1*. RNA prepared from wild-type Col0 (W) or from an individual homozygous for *ysl2-1* (M) was reverse transcribed (+RT) and amplified using primers specific for *YSL3* (as a control for cDNA quality) and *YSL2* (see Experimental procedures). As a control for contaminating genomic DNA, samples of RNA with no reverse transcription step (−RT) were amplified. Molecular weight markers (3, 2.5, 2, 1.5, 1.2, 1, 0.9, 0.8, 0.7, 0.6, and 0.5 kb) are shown in the middle lane.

from *YSL2p:GUS* in roots may reflect the stability of the native *YSL2* mRNA, or alternatively may indicate that the elements of the *YSL2* promoter that enhance root expression under these conditions are missing in the *YSL2p:GUS* construct.

Redundancy of YSL2 function

To examine the *in planta* role of YSL2 further, we sought mutants in which the *YSL2* gene was disrupted. We found a putative T-DNA insertion in *YSL2* (SALK_001348) by screening the sequence-indexed *Arabidopsis* T-DNA insertion lines generated by the Salk Institute Genomic Analysis Laboratory (Alonso *et al.*, 2003). PCR screening and sequencing of the resulting PCR fragment confirmed a T-DNA insertion within *YSL2* exon 4 (Figure 6a), so this allele was designated *ysl2-1*. Homozygous *ysl2-1* mutant individuals were identified, and RT-PCR was used to determine whether *YSL2* mRNA expression had been abolished by the T-DNA insertion (Figure 6b). Homozygous *ysl2-1* mutants had undetectably low levels of *YSL2* mRNA, thus *ysl2-1* is a true knockout allele.

Homozygous *ysl2-1* plants exhibited no overt mutant phenotypes when grown in standard culture conditions, either on plates or in soil. As *YSL2* mRNA levels decrease in response to iron deficiency, we predicted that *ysl2-1* mutant plants might be 'pre-adapted' to this condition, and display resistance to iron deficiency. However, when *ysl2-1* plants were grown under iron deficiency, their growth and appearance were again comparable with wild-type control plants: *ysl2-1* plants were neither more susceptible nor more resistant to growth in low iron. The *ysl2-1* mutants exhibited iron deficiency chlorosis with the same timing, and to the same extent as wild-type control plants. By the same argument, we postulated that *ysl2-1* mutant plants might exhibit resistance to high copper treatment. However, the mutant again exhibited no differences from wild-type plants. Mutant plants were also tested on a medium containing decreased amounts of zinc, manganese and copper. The mutants grew comparably with wild-type controls under all these conditions. The total metal content of *ysl2-1* mutant plants was measured by ICP-MS. The levels of all metals were indistinguishable from those present in the wild-type plants. The lack of effect of the *ysl2-1* mutation in these conditions may reflect functional redundancy within the *Arabidopsis* YSL family.

Localization of the YSL2 protein

All of the AtYSL proteins are predicted to be localized to the plasma membrane, as they lack sequences known to target integral membrane proteins to other organelles. We examined the localization of YSL2 using a YSL2–GFP fusion protein. In the fusion construct (*YSL2:GFP*), the entire *YSL2* gene under 564 bp of its native promoter, was fused in-frame at its C-terminus to GFP. In plants stably transformed with this construct, green fluorescence was observed in leaves and in roots (Figure 7a,b). In both the leaves and roots, fluorescence was most apparent in the vascular tissue, which is consistent with the pattern of expression for *YSL2* deduced using *YSL2p:GUS*. Weak fluorescence was observed in non-vascular cells, especially those adjacent to the veins (not shown). In *YSL2:GFP* plants, fluorescence was strongest in elongated cells within the vasculature, apparently xylem parenchyma. Notably, fluorescence was located exclusively at the edges of these cells, consistent with localization to the plasma membrane (Figure 7). Strikingly, fluorescence was only rarely observed at the apical or basal ends of cells (see Figure 7c for a rare exception), but was instead found almost exclusively on the lateral plasma membranes. This localization implies that YSL2 moves metal–NA complexes laterally within the veins of both leaves and roots.

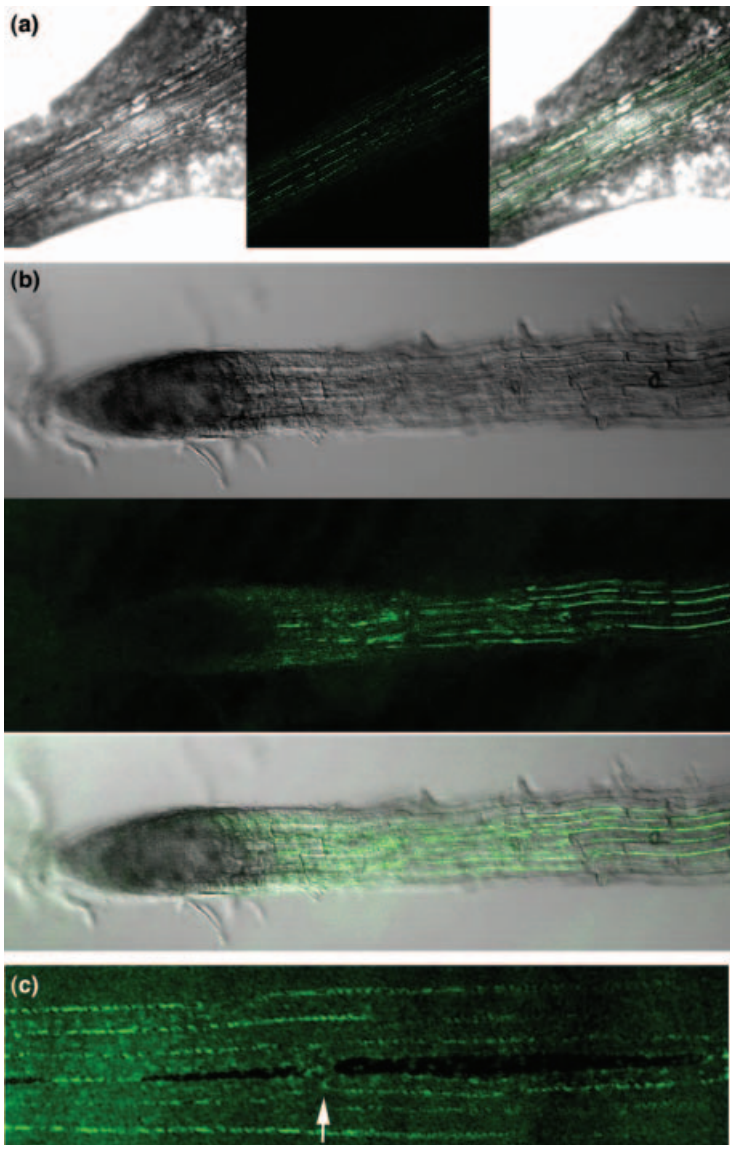

Figure 7. Localization of YSL2:GFP fusion protein.
(a) Optical section through a petiole and lower leaf. Images from left to right are false DIC, fluorescence, and a merged image showing the location of fluorescence.
(b) Optical section through a primary root. Images from top to bottom are as described in (a).
(c) Optical section through a leaf midvein showing a rare instance of fluorescence located at the basal end of a cell.

Discussion

This investigation demonstrates that YSL2 is a transporter of NA-bound metals. YSL2 is capable of transporting Fe–NA and Cu–NA in yeast functional complementation assays. This metal transporter function is further supported by the finding that the patterns of *YSL2* expression change in response to metal concentrations in the surrounding medium. *YSL2* is downregulated by iron limitation and also by copper excess. We have shown that this regulation occurs at the level of transcription as the *YSL2* promoter confers these regulated patterns of expression on a GUS reporter gene.

YSL2 is expressed in many cell types in leaves, roots and reproductive organs. Expression is strongest in the veins, with xylem parenchyma cells having the strongest expression in two reporter constructs. Expression of *YSL2* in non-vascular cells implies that the uptake of iron and copper from NA complexes is accomplished by many cells, not just cells within veins. Furthermore, the finding that *YSL2* is expressed in diverse cell types throughout leaves and roots shows that many cells can take up metals from NA complexes. Moreover, NA must be present within the apoplast in order to provide substrates for YSL2 transport. Thus, in addition to its previously deduced roles in iron solubility within cells, NA also appears to have a significant role as an extracellular chelator of metals.

YSL2:GFP localization is most consistent with a plasma membrane localization for YSL2. However, discerning between plasma membrane and tonoplast membrane localization in the highly vacuolated vascular parenchyma cells that express YSL2 most strongly is difficult, owing to the two membranes being pressed together at the

periphery of these cells. These cells contain plastids, which were readily visible at higher magnifications (not shown), but in no case did we observe a membrane deviating around such a plastid. If YSL2 were located in the tonoplast membrane, we would have expected to see such instances. The localization of YSL2 in membranes at the lateral (but not the apical and basal) ends of the vascular parenchyma cells is also most consistent with the localization of YSL2 to the plasma membrane, as subdomains in the plasma membrane are well documented (Friml *et al.*, 2002a,b; Galweiler *et al.*, 1998; Muller *et al.*, 1998; Swarup *et al.*, 2001), while subdomains of the tonoplast membrane are unknown.

The lateral membrane localization revealed by the YSL2:GFP fusion is consistent with a role in the lateral movement of metals within veins. This lateral movement could be toward or away from the xylem. We hypothesize that the predominant physiologic role for YSL2 is to take up iron that has arrived in tissues via xylem transport, thus moving it away from the xylem vessels. The logic behind this hypothesis rests on YSL2 localization coupled with the pattern of iron-regulated expression observed for *YSL2*. *YSL2* expression is decreased (in both leaves and roots) by iron deficiency. This regulation is in contrast to that of genes that are part of the iron uptake machinery in plants (e.g. *AtIRT1*, *AtFRO2*, and *ZmYS1*). Interestingly, though, the tobacco NA synthase gene is also negatively regulated by iron deficiency (Higuchi *et al.*, 1995).

We hypothesize that the negative regulation of *YSL2* allows the plant to restrict exit of metals from the xylem in roots and mature leaves – the two contexts in which *YSL2* expression is highest. If the role of YSL2 were to move metals toward the xylem, the opposite pattern of expression would be expected, especially in roots, where sparing amounts of iron would need to be mobilized into shoots via the xylem. The restriction of iron exit from the xylem could be interpreted as having either of two opposite consequences. By restricting uptake in mature tissues, metals would continue to be translocated apically toward younger leaves higher on the plant. Conceivably, mature tissues and cells, which already have had time to attain adequate metal levels, can withstand brief periods of iron limitation, while more apical, younger tissues would more rapidly experience metal starvation. Thus downregulation of *YSL2* would represent a mechanism to enhance long-distance iron translocation to shoots by preventing iron sequestration in more basal parts of the plant. Alternatively, the uptake of metals from the xylem stream could represent part of a nutrient cycling mechanism in which metals are passed from the xylem stream into the phloem. In this scenario, preventing the exit of metals from the xylem restricts metal uptake into the phloem, causing metals to remain in mature tissues at the expense of sinks such as the apical meristems and young leaves. It is interesting to note that iron-deficient plants exhibit a pattern of chlorosis in which the veins stay green while the interveinal regions become yellow. It is intriguing to speculate that this pattern reflects iron sequestration within veins that maintains chlorophyll synthesis there.

The finding that *ysl2-1* mutants have no discernible phenotypes, even under conditions of metal deficiency, suggests that other YSL family members confer overlapping functions in metal–NA transport. A functional analysis of other YSL family members is needed to establish whether they have identical biochemical and/or physiologic roles. Moreover, the production of double mutants for those YSLs with apparently overlapping functional roles is expected to shed additional light on the physiologic function(s) performed by the YSL family.

Experimental procedures

Plant growth conditions

Plants were grown in sterile culture on plates containing standard 1X MS medium with 1% sucrose. Seeds were surface sterilized in a solution (20% (v/v) Clorox, 0.01% (v/v) Triton X-100), then imbibed in the dark at 4°C for 3–5 days. Plants were grown at 22°C in a Conviron growth chamber under 16 h day, 8 h night conditions. Pot-grown plants were germinated (following imbibition in the dark at 4°C for 3–5 days) at room temperature under continuous light in 4″ × 4″ pots filled with Promix (Griffin Greenhouse, Tewksbury, MA, USA).

Growth conditions for analysis of the ysl2-1 mutants

Homozygous mutants were grown in standard MS and soil conditions as described above. In addition, these mutants were grown on MS medium modified by independently altering the iron, zinc, manganese, and copper concentrations to 0.5X, 0.25X, 0.1X, and 0X (no added metal). In one trial, the plants were germinated directly on these metal-deficient media; in another, they were germinated on full MS, then transferred after 14 days to metal-deficient plates. In all tests, wild-type ColO plants were grown on the same plate or in the same pot for comparison.

YSL2 cDNA clones

The Ecker size selected (2–3 kB) cDNA library from 3-day hypocotyls was obtained from the Arabidopsis Biological Resource Center. A probe corresponding to the full-length *YSL2* genomic sequence was amplified from *Arabidopsis* genomic DNA, and used to screen the cDNA library. A single full-length clone was identified and was subcloned into the yeast expression vector pFL61 for use in yeast functional complementation assays.

Yeast growth

The iron-uptake-defective strain DEY1453 was grown on standard YPD supplemented with 25 mM NaCitrate (pH 4.2) and 50 μM $FeCl_3$. Once transformed with pFL61-derived plasmids, DEY1453-derived strains were grown on synthetic defined media lacking uracil

supplemented with 25 mM NaCitrate (pH 4.2) and 50 μM $FeCl_3$ (SD-Ura + Fe). For complementation assays, SD-Ura lacking iron was prepared and iron was added, in the forms indicated in the text just prior to pouring plates. Fe(III) and Fe(II) were prepared as 1 M stocks from $FeCl_3$ and $FeSO_4$, respectively, in metal-free RO H_2O. The Fe-containing solutions were immediately sterile filtered and appropriate amounts were added to each plate. Desired volumes of previously prepared sterile NA or MA stock solutions were immediately added to the iron solution. Following complex formation, 15 ml of molten medium was added to the plate, contents were mixed, and plates were allowed to solidify. Yeast cells were diluted and immediately plated onto each freshly prepared medium. Nicotianamine was obtained from T-Hasegawa Co. (Tokyo, Japan). The copper-uptake-defective strain, YSC5 and its transformed derivatives were grown on standard YPD, and standard SD-Ura, respectively. For complementation assays, glycerol was used as a carbon source in place of dextrose and medium was prepared without added copper. Copper was added in the forms indicated in the text just prior to pouring plates.

Semi-quantitative RT-PCR

For the detection of relative transcript abundance by semi-quantitative RT-PCR, total RNA was isolated from 50–75 mg of tissue using the Qiagen RNEasy Kit (Qiagen, Inc., Valencia, CA, USA). Total RNA of 500 ng was used in a reverse transcription reaction with poly d(T) oligo using protocols and reagents from the Invitrogen Superscript RT-PCR System (Invitrogen, Carlsbad, CA, USA). Following DNaseI treatment, 1/10th of the total cDNA reaction was used in a 50-μl polymerase chain reaction using Ex-Taq polymerase (Takara-Mirus, Inc., Madison, WI, USA) for 25 cycles: 94°C, 15 sec, 55°C, 30 sec, 72°C, 1 m 30 sec. These conditions were determined following testing for linear amplification (by analysis of products on ethidium bromide-stained agarose gels) of YSL2 at 17, 19, 21, 23, 25, 27, and 29 cycles. Cycle 25 was found to be within the linear amplification range for YSL2 mRNA in both the root and shoot. The following primer sets were used at a concentration of 0.4 μM in a 50 μl reaction volume: *YSL2*, 5′-caaaaccaacagcatcagcacattgg-3′ (forward), 5′-cgcaaaggcaaagaatccgtagca-3′ (reverse); IRT1, 5′-gagtcattgccatggtcttgga-3′ (forward), 5′-gtatactcagcctggaggatacaaccg-3′ (reverse); *actin*, 5′-gcaagtcatcacgattggtgc-3′ (forward), 5′-gaaccaccgatccagacactgt-3′ (reverse). Amplified products from 15 μl of PCR reaction were visualized on a 1% TAE agarose gel containing ethidium bromide. Bands were photographed using a Kodak Digital Science™ DC40 camera and software (Eastman Kodak, USA).

High sensitivity RT-PCR analysis of ysl2-1

cDNA was prepared from homozygous *ysl2-1* individuals and from wild-type plants as described in the previous section. As a control to detect amplified genomic DNA, RNA that was not reverse transcribed was also amplified. To control for cDNA quality, primers specific for a second *YSL* gene, *YSL3*, were used in a separate set of RT-PCR reactions. We have found that *YSL3* mRNA levels are similar to the levels of *YSL2* mRNA in shoots. The *YSL3* primer set is 5′-attggccaggaaacaagtgtttgggt-3′ (forward) and 5′-gacaagtcccgcgactacaccattt-3′ (reverse). Inclusion of these reactions ensures that failure to observe an amplified *YSL2* cDNA product did not result from poor quality cDNA preparations, but rather from a true absence of mRNA in the mutant plants. PCR was performed in 50 μl reactions using Ex-Taq polymerase (Takara-Mirus, Inc.) for 40 cycles: 94°C, 15 sec, 55°C, 30 sec, 72°C, 1 m 30 sec. Products were visualized as described in the previous section.

GUS histochemical staining and visualization

For analysis of GUS expression under the control of *YSL* promoters, transgenic plants containing *YSL-GUS* reporter constructs were stained in GUS assay buffer [50 mM KPO_4, pH 7.0, 10 mM EDTA, 0.5 mM $K_3Fe(CN)_6$, 0.01% Triton X-100, 0.3 mg ml^{-1} (w/v) X-gluc (5-bromo-4-chloro-3-indolyl β-D-glucuronide; Rose Scientific, CA, USA)] for 2–24 h. Staining was stopped by the addition of 70% (v/v) ethanol. If sectioning was required, plant tissues were fixed with formalin–acetic acid–alcohol (FAA; 50% ethanol, 5% glacial acetic acid, 3.7% formaldehyde in distilled water) for 10 min at room temperature. Destained plants were visualized using a Nikon SMZ1200 dissecting microscope. For thin sections, root and rosette leaf tissues from adult plants were coarse sliced with a razor blade and infiltrated using the Technovit 7100 kit (Kulzer Histo-Technik, Heraeus, Kulzer, Germany). Eight-micron transverse sections were cut using a glass knife and a Microtome Ultracut. Specimens were photographed using a Spot Insight camera and processed with Spot Advanced software (MicroVideo Instruments, Avon, MA, USA) and Adobe Photoshop Version 7.0.

GUS activity measurements

Protein extracts were prepared by grinding tissue in Extraction Buffer (50 mM sodium phosphate, pH 7.0, 10 mM EDTA, 0.1% Triton X-100, 0.1% *N*-lauroylsarcosine, 10 mM β-mercaptoethanol, and 140 μM PMSF), and removing debris by repeated (2×) centrifugation. Extracts were stored at −80°C. Protein concentrations were determined using the Bio-Rad RC DC kit (Bio-Rad, Hercules, CA, USA). GUS activity was measured fluorometrically. Briefly, one-fifth of the total protein extracted was added to GUS assay buffer (50 mM sodium phosphate, pH 7.0, 10 mM EDTA, 0.1% Triton X-100, 0.1% *N*-lauroylsarcosine, 10 mM β-mercaptoethanol, and 50 μM 4-methylumbelliferyl β-D-glucuronide). Half of the assay was immediately removed and quenched in 0.2 M Na_2CO_3, to serve as a control for background fluorescence. The other half was incubated at 37°C for 24 h. Fluorescence was measured in a Turner TBS-380 Minifluorometer (Turner Biosystems, Sunnyvale, CA, USA).

GFP visualization

Seeds were stratified and germinated directly on MS medium, and grown for 2 weeks. Whole plants were visualized using a Zeiss Axiovert confocal microscope using a 488 nm argon laser line, and a 520–550 nm bandpass filter.

Acknowledgements

We thank Satoshi Mori for his very kind gifts of MA and NA, David Salt and Brett Lahner for performing ICP-MS analysis, David Eide and Andy Dancis for generously sharing strains and advice, Joe Ecker for providing his cDNA library, and Tara Burke for diligent technical assistance. We thank Tobias Baskin and Alison DeLong for critical reading of the manuscript.

References

Alonso, J.M., Stepanova, A.N., Leisse, T.J. *et al.* (2003) Genome-wide insertional mutagenesis of *Arabidopsis thaliana*. *Science*, **301**, 653–657.

Anderegg, G. and Ripperger, H. (1989) Correlation between metal complex formation and biological activity of nicotianamine analogues. *J. Chem. Soc. Chem. Commun.* **10**, 647–650.

Askwith, C., Eide, D., Ho, A.V., Bernard, P.S., Li, L., Davis-Kaplan, S., Sipe, D.M. and Kaplan, J. (1994) The *Fet3p* gene of *S. cerevisiae* encodes a multicopper oxidase required for ferrous iron uptake. *Cell*, **76**, 403–410.

Becker, R.F. and Manteuffel, R. (1995) Subcellular localization and characterization of excessive iron in the nicotianamine-less tomato mutant *chloronerva*. *Plant Physiol.* **108**, 269–275.

Becker, R., Grun, M. and Scholz, G. (1992) Nicotianamine and the distribution of iron into the apoplasm and symplasm of tomato (*Lysopersicon exculentum* Mill.). I. Determination of the apoplasmic and symplasmic iron pools in roots and leaves of the cultivar Bonner Beste and its nicotianamine-less mutant *chloronerva*. *Planta*, **187**, 48–52.

Briat, J.F., Lobreaux, S., Grignon, N. and Vansuyt, G. (1999) Regulation of plant ferritin synthesis: how and why. *Cell Mol. Life Sci.* **56**, 155–166.

Cobbett, C. and Goldsbrough, P. (2002) Phytochelatins and metallothioneins: roles in heavy metal detoxification and homeostasis. *Annu. Rev. Plant Biol.* **53**, 159–182.

Curie, C., Panaviene, Z., Loulergue, C., Dellaporta, S.L., Briat, J.F. and Walker, E.L. (2001) Maize *yellow stripe1* encodes a membrane protein directly involved in Fe(III) uptake. *Nature*, **409**, 346–349.

Dancis, A., Haile, D., Yuan, D.S. and Klausner, R.D. (1994a) The *Saccharomyces cerevisiae* copper transport protein (Ctr1p). Biochemical characterization, regulation by copper, and physiologic role in copper uptake. *J. Biol. Chem.* **269**, 25660–25667.

Dancis, A., Yuan, D.S., Haile, D., Askwith, C., Eide, D., Moehle, C., Kaplan, J. and Klausner, R.D. (1994b) Molecular characterization of a copper transport protein in *S. cerevisiae*: an unexpected role for copper in iron transport. *Cell*, **76**, 393–402.

Eide, D., Broderius, M., Fett, J. and Guerinot, M.L. (1996) A novel iron-regulated metal transporter from plants identified by functional expression in yeast. *Proc. Natl Acad. Sci. USA*, **93**, 5624–5628.

Friml, J., Benkova, E., Blilou, I. *et al.* (2002a) AtPIN4 mediates sink-driven auxin gradients and root patterning in *Arabidopsis*. *Cell*, **108**, 661–673.

Friml, J., Wisniewska, J., Benkova, E., Mendgen, K. and Palme, K. (2002b) Lateral relocation of auxin efflux regulator PIN3 mediates tropism in *Arabidopsis*. *Nature*, **415**, 806–809.

Galweiler, L., Guan, C., Muller, A., Wisman, E., Mendgen, K., Yephremov, A. and Palme, K. (1998) Regulation of polar auxin transport by AtPIN1 in *Arabidopsis* vascular tissue. *Science*, **282**, 2226–2230.

Grotz, N., Fox, T., Connolly, E., Park, W., Guerinot, M.L. and Eide, D. (1998) Identification of a family of zinc transporter genes from *Arabidopsis* that respond to zinc deficiency. *Proc. Natl Acad. Sci. USA*, **95**, 7220–7224.

Henrique, R., Jasik, J., Klein, M., Martinoia, E., Feller, U., Schell, J., Pais, M.S. and Koncz, C. (2002) Knock-out of *Arabidopsis* metal transporter gene IRT1 results in iron deficiency accompanied by cell differentiation defects. *Plant Mol. Biol.* **50**, 587–597.

Herbik, A., Koch, G., Mock, H.P., Dushkov, D., Czihal, A., Thielmann, J., Stephan, U.W. and Baumlein, H. (1999) Isolation, characterization and cDNA cloning of nicotianamine synthase from barley. A key enzyme for iron homeostasis in plants. *Eur. J. Biochem.* **265**, 231–239.

Higuchi, K., Nishizawa, N.K., Yamaguchi, H., Romheld, V., Marschner, H. and Mori, S. (1995) Response of nicotianamine synthase activity to Fe-deficiency in tobacco plants as compared with barley. *J. Exp. Bot.* **46**, 1061–1063.

Higuchi, K., Suzuki, K., Nakanishi, H., Yamaguchi, H., Nishizawa, N.K. and Mori, S. (1999) Cloning of nicotianamine synthase genes, novel genes involved in the biosynthesis of phytosiderophores. *Plant Physiol.* **119**, 471–480.

Kruger, C., Berkowitz, O., Stephan, U.W. and Hell, R. (2002) A metal-binding member of the late embryogenesis abundant protein family transports iron in the phloem of *Ricinus communis* L. *J. Biol. Chem.* **277**, 25062–25069.

Lasat, M.M., Pence, N.S., Garvin, D.F., Ebbs, S.D. and Kochian, L.V. (2000) Molecular physiology of zinc transport in the Zn hyperaccumulator *Thlaspi caerulescens*. *J. Exp. Bot.* **51**, 71–79.

Ling, H.Q., Koch, G., Baumlein, H. and Ganal, M.W. (1999) Map-based cloning of chloronerva, a gene involved in iron uptake of higher plants encoding nicotianamine synthase. *Proc. Natl Acad. Sci. USA*, **96**, 7098–7103.

Liu, D.H., Adler, K. and Stephan, U.W. (1998) Iron-containing particles accumulate in organelles and vacuoles of leaf and root cells in the nicotianamine-free tomato mutant *chloronerva*. *Protoplasma*, **201**, 213–220.

Minet, M., Dufour, M.E. and Lacroute, F. (1992) Complementation of Saccharomyces cerevisiae auxotrophic mutants by *Arabidopsis thaliana* cDNAs. *Plant J.* **2**, 417–422.

Muller, A., Guan, C., Galweiler, L., Tanzler, P., Huijser, P., Marchant, A., Parry, G., Bennett, M., Wisman, E. and Palme, K. (1998) AtPIN2 defines a locus of *Arabidopsis* for root gravitropism control. *EMBO J.* **17**, 6903–6911.

Pence, N.S., Larsen, P.B., Ebbs, S.D., Letham, D.L., Lasat, M.M., Garvin, D.F., Eide, D. and Kochian, L.V. (2000) The molecular physiology of heavy metal transport in the Zn/Cd hyperaccumulator *Thlaspi caerulescens*. *Proc. Natl Acad. Sci. USA*, **97**, 4956–4960.

Persson, B. and Argos, P. (1994) Prediction of transmembrane segments in proteins utilising multiple sequence alignments. *J. Mol. Biol.* **237**, 182–192.

Persson, B. and Argos, P. (1996) Topology prediction of membrane proteins. *Protein Sci.* **5**, 363–371.

Pich, A. and Scholz, G. (1991) Nicotianamine and the distribution of iron into apoplast and symplast of tomato (*Lycopersicon esculentum* Mill.). II. Uptake of iron by protoplasts from the variety Bonner Beste and its nicotianamine-less mutant chloronerva and the compartmentation of iron in leaves. *J. Exp. Bot.* **42**, 1517–1523.

Pich, A. and Scholz, G. (1996) Translocation of copper and other micronutrients in tomato plants (*Lycopersicon exculentum* Mill.): nicotianamine-stimulated copper transport in the xylem. *J. Exp. Bot.* **47**, 41–47.

Pich, A., Scholz, G. and Stephan, U.W. (1994) Iron-dependent changes of heavy metals, nicotianamine, and citrate in different plant organs and in the xylem exudate of two tomato genotypes. Nicotianamine as possible copper translocator. *Plant Soil*, **165**, 189–196.

Reichman, S.M. and Parker, D.R. (2002) Revisiting the metal-binding chemistry of nicotianamine and 2′-deoxymugineic acid. Implications for iron nutrition in strategy II plants. *Plant Physiol.* **129**, 1435–1438.

Roberts, L.A., Pierson, A.J., Panaviene, Z. and Walker, E.L. (2004) Yellow Stripe 1. Expanded roles for the Maize iron-phytosiderophore transporter. *Plant Physiol.* **135**, 112–120.

Robinson, N.J., Procter, C.M., Connolly, E.L. and Guerinot, M.L. (1999) A ferric-chelate reductase for iron uptake from soils. *Nature*, **397**, 694–697.

Schaaf, G., Ludewig, U., Erenoglu, B.E., Mori, S., Kitahara, T. and Wirén, N.v. (2004) ZmYS1 functions as a proton-coupled symporter for phytosiderophore- and nicotianamine-chelated metals. *J. Biol. Chem.* **279**, 9091–9096.

Schmidke, I. and Stephan, U.W. (1995) Transport of metal micronutrients in the phloem of castor bean (*Ricinus communis*) seedlings. *Physiol. Plant.* **95**, 147–153.

Stephan, U.W. and Grun, M. (1989) Physiological disorders of the nicotianamine-auxothroph tomato mutant *chloronerva* at different levels of iron nutrition. II. Iron deficiency response and heavy metal metabolism. *Biochem. Physiol. Pflanzen*, **185**, 189–200.

Stephan, U.W., Scholz, G. and Rudolph, A. (1990) Distribution of nicotianamine, a presumed symplast iron transporter, in different organs of sunflower and of a tomato wild type and its mutant *chloronerva*. *Biochem. Physiol. Pflanzen*, **186**, 81–88.

Swarup, R., Friml, J., Marchant, A., Ljung, K., Sandberg, G., Palme, K. and Bennett, M. (2001) Localization of the auxin permease AUX1 suggests two functionally distinct hormone transport pathways operate in the *Arabidopsis* root apex. *Genes Dev.* **15**, 2648–2653.

Thomine, S., Lelievre, F., Debarbieux, E., Schroeder, J.I. and Barbier-Brygoo, H. (2003) AtNRAMP3, a multispecific vacuolar metal transporter involved in plant responses to iron deficiency. *Plant J.* **34**, 685–695.

Varotto, C., Maiwald, D., Pesaresi, P., Jahns, P., Salamini, F. and Leister, D. (2002) The metal ion transporter IRT1 is necessary for iron homeostasis and efficient photosynthesis in *Arabidopsis thaliana*. *Plant J.* **31**, 589–599.

Vert, G., Grotz, N., Dedaldechamp, F., Gaymard, F., Guerinot, M.L., Briat, J.F. and Curie, C. (2002) IRT1, an *Arabidopsis* transporter essential for iron uptake from the soil and for plant growth. *Plant Cell*, **14**, 1223–1233.

von Wiren, N., Klair, S., Bansal, S., Briat, J.-F., Khodr, H., Shioiri, T., Leigh, R.A. and Hider, R.C. (1999) Nicotianamine chelates both Fe[III] and Fe[II]. Implications for metal transport in plants. *Plant Physiol.* **119**, 1107–1114.

Zhao, H. and Eide, D. (1996) The ZRT2 gene encodes the low affinity zinc transporter in Saccharomyces cerevisiae. *J. Biol. Chem.* **271**, 23203–23210.

Zhou, B. and Gitschier, J. (1997) hCTR1: a human gene for copper uptake identified by complementation in yeast. *Proc. Natl Acad. Sci. USA*, **94**, 7481–7486.